PHYSICAL REVIEW B VOLUME 23, NUMBER 8 15 APRIL 1981

A study of the H/W(110) adsorption system by surface reflectance spectroscopy

Graciela B. Blanchet,* P. J. Estrup, and P. J. Stiles
Department of Physics, Brown University, Providence, Rhode Island 02912
(Received 12 November 1980)

A method for the analysis of surface reflectance spectroscopy data is presented and applied to hydrogen chemisorbed on tungsten (110). This system is found to have highly anisotropic optical properties. The angular dependence of the more prominent features in the dielectric function is predicted for different structural models. The transition matrix elements are calculated with a tight-binding approximation after restricting the set of wave functions by using symmetry arguments and dipole-moment selection rules. A comparison with the experimental data determines the symmetry of the adsorbate wave functions and shows that the most likely adatom position is in a bridged site. The direct optical transitions are identified and the location of the resonance levels and adsorbate states in the surface band structure is determined.

I. INTRODUCTION

In studies of surface band structure in transition metals special attention is given to those experimental techniques that allow a direct comparison between theoretical and experimental results. Surface reflectance spectroscopy[1-5] (SRS) and ultraviolet photoemission spectroscopy[6,7] (UPS) are among the most useful techniques for this purpose because they are intrinsicly sensitive to the surface electronic properties.

In integrated photoemission experiments[6,7] electrons leaving the surface at almost all angles are collected. The results give information about the average energy position in the surface Brillouin zone (SBZ) of an electronic state. In angle-resolved UPS experiments[8,9] the azimuthal and polar electron collection angles can be varied, and as a result it is possible to select a particular region of the SBZ to be studied. These latter studies give a rather complete description of the surface band structure below the Fermi level (E_F). Surface reflectance spectroscopy, on the other hand, gives information about the electronic states located between E_F and E_v (the vacuum level). The two techniques when used together are suitable for testing calculated surface band structures. SRS is a highly sensitive optical technique which previously has been used mainly in electrochemical investigations.[10] It was applied some years ago to the study of the small changes in reflectance, $\Delta R/R$, that occur when atoms or molecules are chemisorbed on an atomically clean surface.[1,2] The presence of the adsorbate modified the electronic structure at the surface region causing changes in reflectance that are measured as a function of the incident photon energy. The electronic structure at the interface is obtained from the dielectric response of the system, which in turn is deduced from the $\Delta R/R$ spectra.[1,2,11] In particular cases, measurements of the coverage dependence of $\Delta R/R$ at fixed photon energies can be useful in characterizing individual binding states.

The analysis of SRS data that is presented here permits the characterization of features in the surface band structure and the determination of the bonding configuration of the adsorbate. The system studied, hydrogen chemisorbed on tungsten (110), is found to have highly anisotropic optical properties[12]; thus, the reflectivity change, $\Delta R/R$, depends strongly on the azimuthal orientation of the electric field. Similar anisotropies in the optical properties have also been observed for the O/W(110) (Ref. 12) and Cu/Pd (110) (Ref. 13) systems.

Two groups of experiments, described in detail in Sec. III, are necessary to describe the H/W (110) system. The dependence of $\Delta R/R$ on the azimuthal direction of the electric field, at fixed photon energy, gives the symmetry properties of the clean and adsorbate-covered tungsten surface. From these data the principal directions of the dielectric tensor are identified. In the other experiments the spectral dependence of $\Delta R/R$ is measured with the electric field along the principal directions of the dielectric tensor; these results give the electronic properties in the surface region.

As shown in Sec. IV, the anisotropy in the optical properties results from remarkably different dielectric functions for an electric field along each principal direction. The amplitude of a peak in the imaginary part of the dielectric functions, $\Delta\epsilon_2$, is proportional to the square of the matrix element of the dipole moment operator in the direction of the electric field between the initial- and final-state electronic wave functions. By changing the direction of the electric field, the matrix element changes because the strength of the optical transitions varies due to the directionality of the wave functions that participate in the

bonding. For the calculation of the matrix elements we identify the set of wave functions associated with a particular adsorbate geometry. A group-theoretical treatment gives the allowed mixing of the hydrogen and tungsten orbitals along the high symmetry lines in the SBZ. The dipole moment selection rules further restrict the electronic states that participate in a direct optical transition. The transition matrix elements are then calculated within a tight-binding approximation for different model configurations of the adsorbate. Then the angular dependence of the calculated matrix elements is compared to that obtained experimentally until a particular H geometry can fit the data. In the analysis, the direct optical transitions are identified and located in the projected band structure (PBS) of the (110) SBZ.

II. EXPERIMENTAL PROCEDURES

The single-crystal sample was a thin ribbon of tungsten with its surface oriented to within $\frac{1}{2}°$ of the {110} plane. It was mounted in an ultrahigh vacuum (UHV) chamber with a background pressure in the low 10^{-10}-Torr range. The hydrogen was admitted to the chamber through leak valves and monitored with a partial-pressure analyzer. Resistive heating of the sample to 2200 °C, for a short period of time, usually produced an atomically clean surface but occasional heating in oxygen was necessary to eliminate carbon contamination. Auger electron spectra indicated that this cleaning procedure was adequate.

The experiments were performed at near-normal incidence ($\theta \leq 1°$), so that the electric field was always tangential to the surface plane (s-polarized light). All possible polarizations, ϕ, were obtained by rotating a polaroid in the {110} plane.

A double-beam spectrometer,[11,14] shown in Fig. 1, was used to measure the changes of reflectance ($\Delta R \simeq 10^{-3} R$). Light either from an unpolarized tungsten-halogen source ($\hbar\omega \leq 4.8$ eV) or from a low-pressure deuterium discharge (4.8 eV $\leq \hbar\omega \leq 6.0$ eV) was passed through a prism monochromator and a polarizer to select wavelength and polarization. The light beam in the spectrometer was divided into two by a CaF_2 beam splitter. One of the beams was reflected at $\leq 1°$ with respect to the normal of the W(110) sample located in the UHV chamber, and the other beam was reflected from a tungsten reference sample located outside the chamber. These two beams were chopped by a pair of tuning forks approximately 180° out of phase and focused onto the detector.

As shown in the inset of Fig. 1, the detector received alternatively the sample signal ($R_s I_0$) and the reference signal ($R_r I_0$). A lead sulfide detector and different photomultipliers were used in the near ir spectral region (0.5 eV $\leq \hbar\omega \leq 1.5$ eV) and in the visible uv region (1.5 eV $\leq \hbar\omega \leq 6.0$ eV), respectively. A feedback mechanism[15] adjusted the photomultiplier gain to maintain the reference signal at 1 V, thereby normalizing the change of reflectance.

The difference in reflectance between the clean W(110) sample and the reference sample was measured continuously as a function of photon energy for a fixed azimuthal orientation ϕ of the electric field. The reference and sample voltages were electronically subtracted and the difference recorded in a multichannel analyzer as a function of photon energy.

Hydrogen was then admitted into the UHV cham-

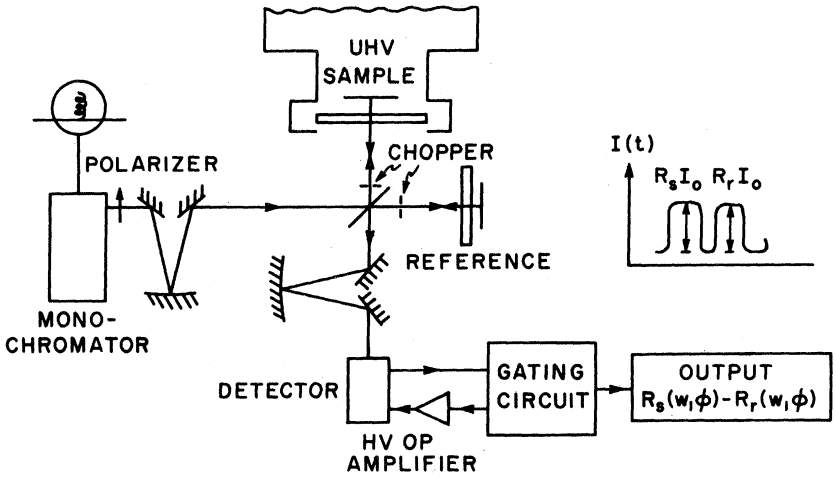

FIG. 1. Schematic diagram of the experimental system.

ber until the W(110) surface was saturated. The change in reflectance between the hydrogen-covered sample and the reference sample was obtained as before and recorded as a function of photon frequency. This latter difference was digitally subtracted from the former to obtain the spectral dependence of the normalized change of reflectance $\Delta R/R$. This quantity was measured in the same spectral region for 19 different azimuthal orientations of the electric field, which was varied in intervals of 5° from $\phi = 0°$ ($\langle 1\bar{1}0\rangle$ direction) to $\phi = 90°$ ($\langle 001\rangle$ direction).

In these SRS experiments, the noise level and the zero offsets are critical problems that can be minimized by reducing the difference in optical path between sample and reference beams. An additional complication is that, with the optical arrangement shown in Fig. 1, the beam splitter introduces strong polarization effects. For small azimuthal angles the transmitted beam is more intense than the reflected beam. For large values of ϕ the intensity of the reflected beam increases. As a result, it was not possible to sweep the polarization continuously at fixed photon energy. The beam splitter polarization effects are 100 times as large as the change in reflectance. To minimize the difference in the optical path between reference and sample beams, the intensity of the strongest beam was attenuated by introducing a shutter in the path of the beam.

To reduce the noise level without losing intensity, the data were statistically averaged over 16 successive runs. The resulting uncertainty in $\Delta R/R$ was 5% in the visible uv region and of the order of 10% in the ir region.

III. RESULTS

The anisotropy in the optical properties of H/W (110) was determined from the dependence of $\Delta R/R$ on the azimuthal orientation (ϕ) of the electric field.

Polar plots of $\Delta R/R$ as a function of ϕ at different values of the photon energy are shown in Fig. 2. These curves have very different shapes in the energy range studied. The dots are the experimental data and the curves represent the fitting to a relation of the form $A + B\cos^2\phi$, where A and B are frequency-dependent coefficients. It was found that $A = \Delta R/R\ \langle 001\rangle$ and $B = \Delta R/R\ \langle 001\rangle - \Delta R/R\ \langle 1\bar{1}0\rangle$. These results show that the $\langle 100\rangle$ and $\langle 1\bar{1}0\rangle$ directions are the principal axes of the surface dielectric tensor.

The same conclusion can be obtained from a classical electrodynamics treatment.[16,17] We start with the Maxwell equations for a semi-infinite system described by a nonlocal dielectric tensor $\bar{\epsilon}(\vec{r},\vec{r}',\omega)$:

$$\vec{\nabla}(\vec{\nabla}\cdot\vec{E}) - \nabla^2\vec{E} = \int \bar{\epsilon}(\vec{r},\vec{r}',\omega)\vec{E}(\vec{r}')d^3r'. \tag{1}$$

In Eq. (1) the electric field is $\vec{E}(\vec{r},t) = \vec{E}_0 e^{i(\vec{q}\cdot\vec{r}-\omega t)}$ and the wave vector $\vec{q}$ is $(0,0,q_z)$. Thus the electric field $\vec{E}(\vec{r},t)$ is $(E_x(z),E_y(z),0)e^{i\omega t}$, where z is chosen to be normal to the surface. If (x,y) are the pair of orthogonal axes that diagonalize the dielectric tensor in the surface region, Eq. (1) can be written as two uncoupled equations:

$$\begin{aligned} -\frac{\partial^2 E_x(z)}{\partial z^2} &= \frac{\omega^2}{c^2}\int \epsilon^{xx}(\vec{r},\vec{r}',\omega)E_x(z)d^3r', \\ -\frac{\partial^2 E_y(z)}{\partial z^2} &= \frac{\omega^2}{c^2}\int \epsilon^{yy}(\vec{r},\vec{r}',\omega)E_y(z)d^3r'. \end{aligned} \tag{2}$$

The asymptotic solutions of Eq. (2) are found by using the scalar Green's-function method, following a procedure similar to that described in Ref. (17) for p-polarized light. The result is

$$E_x(z\to-\infty) \propto E_x^0(e^{iqz} - r_x e^{-iqz}),$$

$$E_y(z\to-\infty) \propto E_y^0(e^{iqz} - r_y e^{-iqz}).$$

From classical electrodynamics, the reflectivity at the surface region can be expressed as

$$\begin{aligned} R_s = \left|\frac{E^{\mathrm{ref}}}{E_0}\right|^2 &= (r_x)^2\cos^2\phi + (r_y)^2\sin^2\phi \\ &= (R_{\mathrm{bk}} + \Delta R_x^s)\cos^2\phi + (R_{\mathrm{bk}} + \Delta R_y^s)\sin^2\phi. \end{aligned}$$

ΔR_x^s and ΔR_y^s, in the above equation, are the corrections to the bulk reflectance due to the presence of a surface. The normalized change in reflectance at the surface can be written as

$$\frac{\Delta R^s}{R} = \frac{R_s - R_{\mathrm{bk}}}{R_{\mathrm{bk}}} = \frac{\Delta R_x^s}{R}\cos^2\phi + \frac{\Delta R_y^s}{R}\sin^2\phi. \tag{3}$$

One can treat the adsorbate-covered surface in a similar manner. Let (a,b) be the pair of orthogonal axes in which the dielectric tensor for the chemisorption case is diagonal. These axes are rotated by angle ξ in the surface plane with respect to the (x,y) axes. By repeating the procedure used for the clean surface, the correction to the bulk reflectance due to the adsorbate-covered surface is

$$\frac{\Delta R^{\mathrm{ch}}}{R} = \frac{R_{\mathrm{ch}} - R_{\mathrm{bk}}}{R_{\mathrm{bk}}} = \frac{\Delta R_a^{\mathrm{ch}}}{R}\cos^2(\xi-\phi) + \frac{\Delta R_b^{\mathrm{ch}}}{R}\sin^2(\xi-\phi). \tag{4}$$

The measured quantity is the difference in reflectance between the clean and adsorbate-covered surface and can be written as

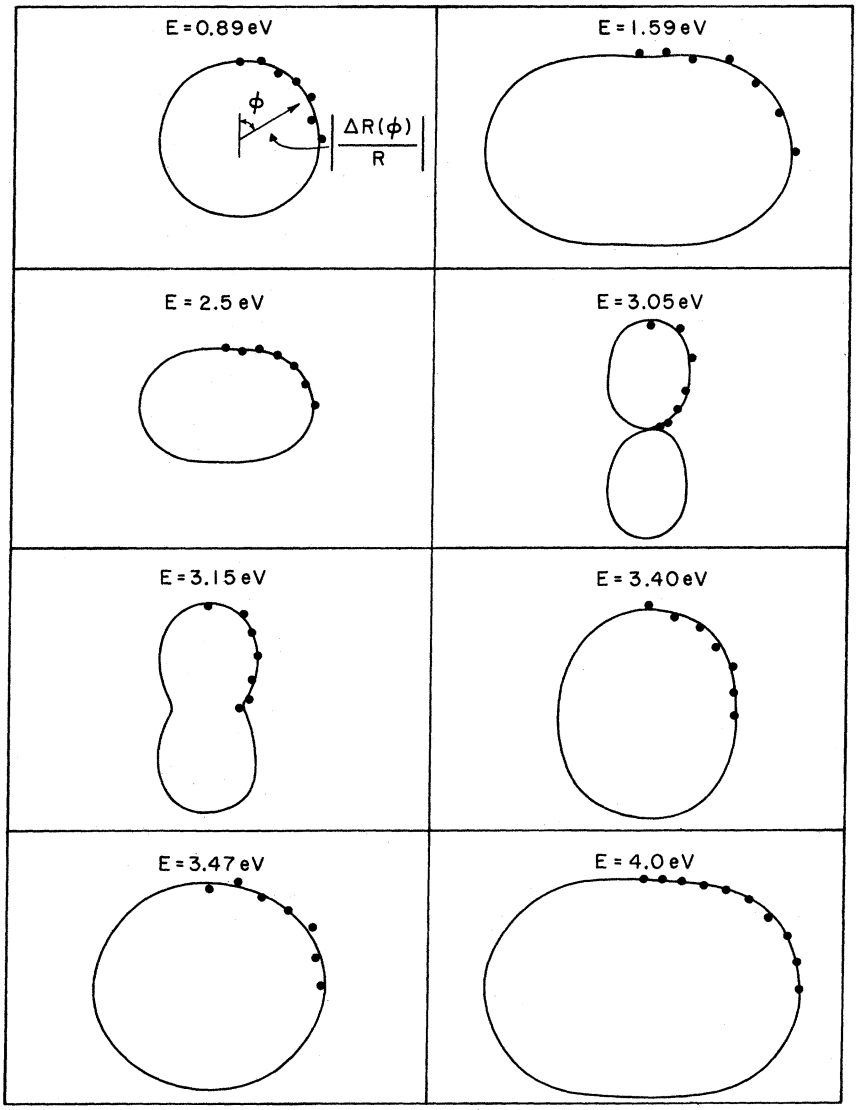

FIG. 2. Polar plot of $\Delta R/R$ as a function of the azimuthal orientation of the electric field for different photon energies. The dots refer to the experimental points. The solid line curves are the fits to $A+B\cos^2\phi$.

$$\frac{\Delta R}{R}(\phi,\omega)=\left(\frac{\Delta R_b}{R}-\frac{\Delta R_y}{R}\right)+\left(\frac{\Delta R_a}{R}-\frac{\Delta R_b}{R}\right)\cos^2(\xi-\phi)+\left(\frac{\Delta R_y}{R}-\frac{\Delta R_x}{R}\right)\cos^2\phi. \quad (5)$$

An expression of the form of Eq. (5) cannot fit the data unless $\xi=0°\,[(x,y)\equiv(a,b)]$. Under such conditions, Eq. (5) reduces to

$$\frac{\Delta R}{R}(\phi,\omega)=\frac{\Delta R_y}{R}+\left(\frac{\Delta R_x}{R}-\frac{\Delta R_y}{R}\right)\cos^2\phi. \quad (6)$$

Comparison between the experimental expression and Eq. (6) shows that the $\langle 001\rangle$ and the $\langle 1\bar{1}0\rangle$ directions are the principal axes of the dielectric tensor for both the clean and hydrogen-covered tungsten surface. Evidently, hydrogen does not cause rotation of the principal axes of the surface dielectric tensor, i.e., the symmetry of the clean surface remains unchanged. Since both the clean and the adsorbate-covered surface have rectangular symmetry, all overlayer configurations without such symmetry may be rejected as possible models for the surface geometry. It is evident from Eq. (6) that the frequency dependence of $\Delta R/R$ for an electric field along one of the principal axes of the tensor is sufficient information to describe the dielectric response of the system.

The spectral dependence of $\Delta R/R$ for an electric field along the $\langle 1\bar{1}0\rangle$ direction and the $\langle 001\rangle$ direction are shown in Fig. 3. In the analysis

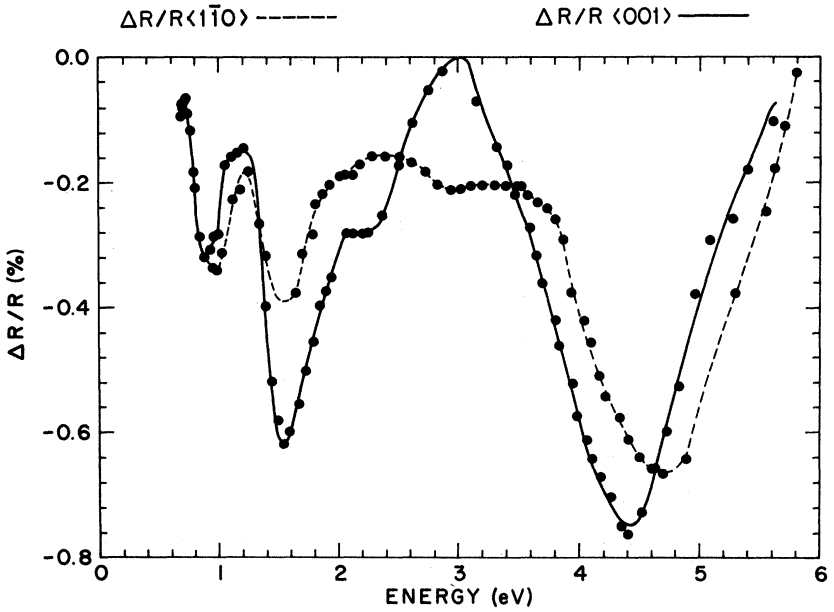

FIG. 3. Dependence of the normalized change of reflectance $\Delta R/R(\omega)$ on photon energy for a W(110) surface saturated with hydrogen at room temperature. The electric field is along the $\langle 1\bar{1}0\rangle$ and $\langle 001\rangle$ directions.

of the reflectivity spectra, two separate regions are considered: the near ir region ($0.6\ \text{eV} < \hbar\omega < 1.5\ \text{eV}$) and the visible-uv region ($1.5\ \text{eV} < \hbar\omega < 6.0\ \text{eV}$). In the near ir region, the amplitude of the structure is seen to depend on the azimuthal orientation of the electric field. However, the energy position of the features is independent of the direction of the electric field. In contrast, the curves are remarkably different in the visible uv region. $\Delta R/R$ ⟨001⟩ shows a maximum at 3.0 eV, a minimum at 5.0 eV, and a shoulder at 2.6 eV. On the other hand, $\Delta R/R$ $\langle 1\bar{1}0\rangle$ is essentially structureless up to 3.4 eV after which it decreases monotonically to a minimum at 5.5 eV. The differences between the spectra show the sensitivity of SRS to small surface anisotropies.

In order to obtain information about the surface electronic structure, it is necessary to relate the measured changes in reflectance to changes in the dielectric response. The classical model of McIntyre and Aspnes[18] (MA) has been widely used to study the dielectric properties of chemisorption systems. It has been shown[16] that the MA model is a very good approximation for s polarization and an isotropic interface.

Feibelman calculated an expression for $\Delta R/R$ in terms of a local dielectric function,[16] and his treatment can be extended to the case of an anisotropic interface. For s-polarized light, the electric field is purely tangential to the surface. As a consequence of the classical boundary conditions, the field must vary slowly across the surface region. Therefore, it is a good approximation to reduce the nonlocal conductivity tensor to a local one. The change in reflectance can then be expressed as[16]

$$\left.\frac{\Delta R_x^s}{R}\right|_{\text{micr}} = 4q\int_0^d dz\,\text{Im}\left(\frac{\sigma_{\text{loc}}^x(z)}{\sigma_{\text{loc}}^x(\infty)}\right),$$
$$\left.\frac{\Delta R_y^s}{R}\right|_{\text{micr}} = 4q\int_0^d dz\,\text{Im}\left(\frac{\sigma_{\text{loc}}^y(z)}{\sigma_{\text{loc}}^y(\infty)}\right), \tag{7}$$

where

$$\vec{\sigma}_{\text{loc}}(\vec{r}) = \int \vec{\sigma}(\vec{r},\vec{r}')d^3r' .$$

The local dielectric function is a smoothly varying function across the interface. It is therefore reasonable to replace it by its mean value. This approximation leads to a McIntyre and Aspnes type expression[18] for each principal direction of the dielectric tensor:

$$\left.\frac{\Delta R^x}{R}\right|_{\text{class}} = 4qd\,\text{Im}\left(\frac{\sigma_s^x}{\sigma_{\text{bk}}}\right),$$
$$\left.\frac{\Delta R^y}{R}\right|_{\text{class}} = 4qd\,\text{Im}\left(\frac{\sigma_s^y}{\sigma_{\text{bk}}}\right). \tag{8}$$

The measured quantities, the difference in reflectance between an adsorbate-covered and a clean surface, can be written in general as

$$\frac{\Delta R^x}{R} = -\frac{8\pi d}{\lambda}\cos\theta_i\left(\frac{\epsilon_{2b}\Delta\epsilon_1^x + (\epsilon_{1b}-1)\Delta\epsilon_2^x}{(1-\epsilon_{1b})^2+\epsilon_{2b}^2}\right), \tag{9a}$$

$$\frac{\Delta R^y}{R} = -\frac{8\pi d}{\lambda}\cos\theta_i\left(\frac{\epsilon_{2b}\Delta\epsilon_1^y + (\epsilon_{1b}-1)\Delta\epsilon_2^y}{(1-\epsilon_{1b})^2+\epsilon_{2b}^2}\right). \tag{9b}$$

In Eqs. (9) $\epsilon_{bk}=\epsilon_{1b}+i\epsilon_{2b}$ is the bulk dielectric function[19] and $\Delta\epsilon=\Delta\epsilon_1+i\Delta\epsilon_2$ are the changes in a local, average, surface dielectric function for an electric field along the x or the y direction.

In each of the Eqs. (9), two unknowns appear: the real and the imaginary parts of the change in the dielectric function. However, they are not independent but are related to each other by the Kramers-Kronig dispersion relations.[20] It is convenient to represent $\Delta\epsilon(\omega)$ by a function that automatically fulfills the dispersion relations and contains a minimum of free parameters to fit the experimental data. It is assumed that $\Delta\epsilon$ can be represented, along each principal direction, by a sum of Lorentzians. The oscillator parameters are than computer-adjusted to reproduce the experimental spectra.[2,11,14] However, the Lorentzian parameters that result from the fitting do not have any particular physical meaning.[11] It is found that different sets of oscillator parameters can give an equally good fit to the data and can produce similar structure in $\Delta\epsilon_2(\omega)$,

The dielectric functions obtained for H/W(110) are shown in Fig. 4. It is important to consider the effect that the sum rule imposed on the oscillator strengths ($\sum_j f_j = S$) has on the resulting dielectric function. Figure 5 shows two dielectric functions obtained with very different S, the values being approximately 0 and 200, respectively. Both give an equally good fit to the experimental data. A surface sum of about 50 is obtained from the expression given by Restorff *et al.*[21] Comparison of the curves in Fig. 5 shows that neither the energy position of the structure nor the dispersion of the peaks change. However, the relative strength of the peaks depends strongly on S. For all the values of S considered, the amplitude of the low-energy structure decreases and the amplitude of the high-energy features increases when S is lowered.

The dielectric functions shown in Fig. 4 resulted from a value of S about 100. The high value of S causes negative structure, such as the dip at 1.4 eV, to appear positive. However, an analysis of the electronic properties requires a comparison of the $\Delta\epsilon_2$ curves for different orientations of the electric field. For this purpose, both curves must obey the same sum rule. In Fig. 4 they do and the relative strength of the peaks can then be compared.

$\Delta\epsilon\ \langle 1\bar{1}0\rangle$ was compared to the one obtained by Restorff[21] from a Kramers-Kronig analysis. Agreement is found, as expected, with the energy position of all peaks.

The real part of the changes in dielectric functions are shown in Fig. 6. The changes in the joint density of states, $\Delta J_{if}(\omega)$, were calculated

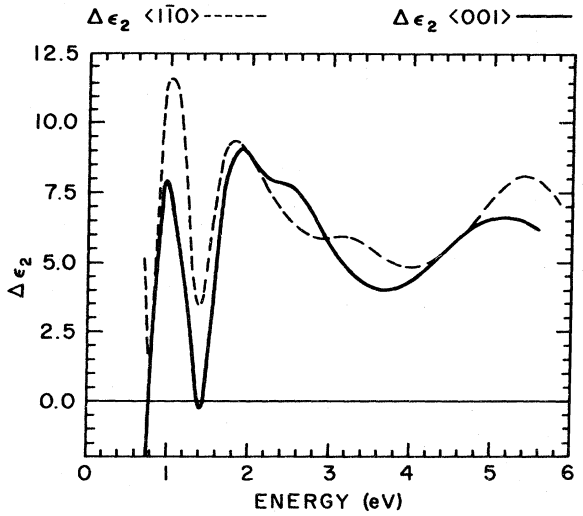

FIG. 4. Frequency dependence of the change in the imaginary part of the dielectric functions caused by hydrogen adsorption. The electric field is along the $\langle 1\bar{1}0\rangle$ and the $\langle 001\rangle$ directions.

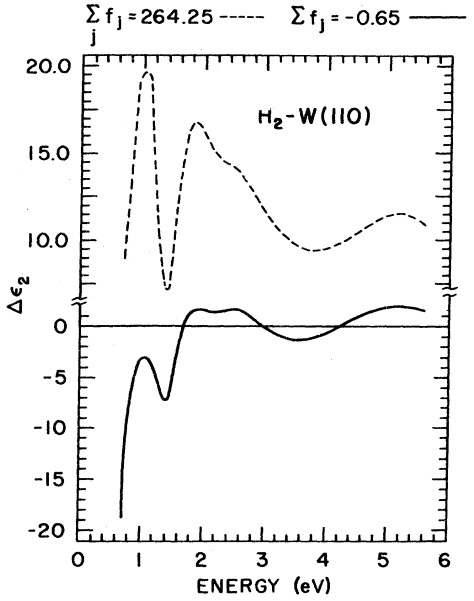

FIG. 5. Spectral dependence of the change in the imaginary part of the dielectric function for two very different sum rules. The electric field is along the $\langle 001\rangle$ direction.

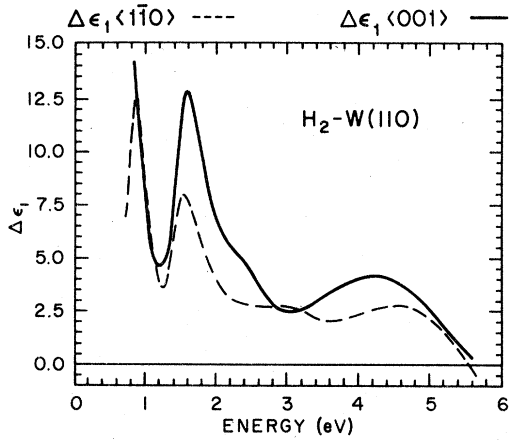

FIG. 6. Spectra of the changes in the real part of the surface dielectric function caused by a monolayer of H chemisorbed at room temperature. The electric field is along the ⟨001⟩ and the ⟨1$\bar{1}$0⟩ directions.

by assuming a constant matrix element for an electric field along the principal axis of the dielectric tensor ($\Delta J_{if}\langle 100\rangle = \omega^2 \Delta\epsilon_2 \langle 100\rangle$). The resulting spectral curves are shown in Fig. 7 for the electric field along the ⟨001⟩ and the ⟨1$\bar{1}$0⟩ directions.

IV. DISCUSSION

A. Dielectric response and electronic properties

The structure in $\Delta\epsilon_2(\omega)$ (Fig. 4) for the electric field along the ⟨1$\bar{1}$0⟩ and ⟨001⟩ directions was analyzed as described below. The imaginary part of the dielectric function is directly related to the absorption spectrum of the system. The sign, energy position, and amplitude of the peaks in

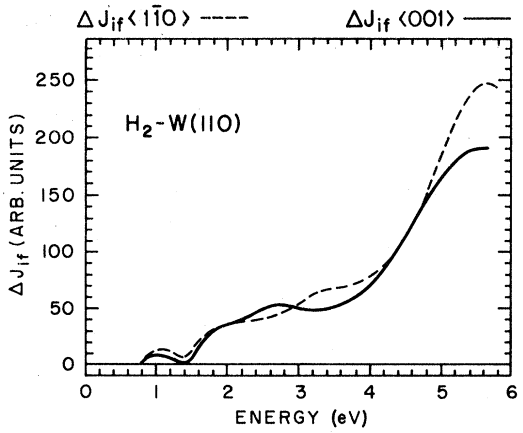

FIG. 7. W(110) changes of the joint density of states ($\Delta J_{if}\langle 001\rangle = \omega^2 \Delta\epsilon_2 \langle 001\rangle$ and $\Delta J_{if}\langle 1\bar{1}0\rangle = \omega^2 \Delta\epsilon_2 \langle 1\bar{1}0\rangle$).

$\Delta\epsilon_2$ give information about energies and wave functions of the electronic states as well as the geometry of the adsorbate on the surface plane.[12]

The structure that appears in the bulk dielectric function is always positive; however, the structure in $\Delta\epsilon_2$ can be positive or negative. A positive contribution indicates that the strength of an optical transition increases with chemisorption. Thus a peak in $\Delta\epsilon_2$ shows that either new states appear (i.e., adsorbate-induced features) or that the strength of the optical transition between electronic states characteristic of the clean surface increases upon adsorption. A minimum in the dielectric function indicates that the strength of transitions involving states characteristic of the surface decreases with adsorption. Finally, a dip in $\Delta\epsilon_2$ is associated with the quenching upon adsorption of surface states or resonance levels.

When a solid is excited by light of the appropriate frequency, there is a transition from an occupied electronic state with energy E_i to an unoccupied state with energy E_f. Their energy difference is an excitation energy of the system and its corresponds directly to the position of a peak in $\Delta\epsilon_2$. The width of such a peak is related to the dispersion and the lifetime of the initial and final electronic states.

The amplitude of a peak in $\Delta\epsilon_2$ is a measure of the strength of the optical transition, and it is proportional to the squared matrix element of the appropriate dipole-moment operator between the initial and final states.[12] Consequently, one can describe the system by analyzing the position, width, and amplitude of the peaks and minima in $\Delta\epsilon_2$.

The information contained in a $\Delta\epsilon_2$ curve can be analyzed in terms of direct optical transitions in the surface band structure under consideration. The wave functions associated with an electronic state can be determined if one identifies first the region of the surface Brillouin zone (SBZ) where the state is located. If it appears along particular lines in the SBZ, symmetry considerations restrict the possible orbital character of the wave functions that can be associated with the electronic state.

The surface band structure (Fig. 8) was obtained by projecting the bulk band structure calculated by Christensen and Feuerbacher[22] onto the ⟨110⟩ SBZ. Although a band structure obtained in this way does not give any information about localized states (surface and resonance levels), it does give the position of the gaps and bands. This knowledge is necessary because a gap or a region of low density of states is a favorable location for the localized states that appear when

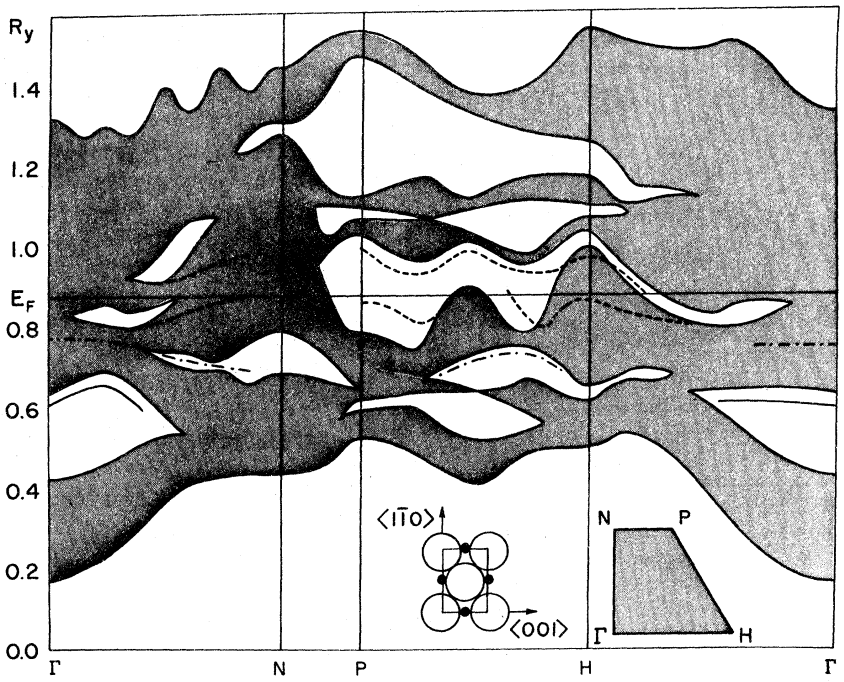

FIG. 8. Projected band structure for the W(110) surface. Dashed lines refer to the surface resonances, solid lines to the high-coverage hydrogen state and dashed-dotted lines to the low-coverage hydrogen state. Insets show the corresponding SBZ and the bridge-site position of the atoms (solid circles) on the direct W lattice (empty circles).

the translational symmetry is broken due to the presence of the surface. The projected band structure (PBS) (Fig. 8) shows a continuum of states whose wave functions, associated with the band states, extend deep into the bulk. In contrast, the wave functions of surface and adsorbate states are highly localized in the surface region.[23,24]

Any pair of band, resonance, and adsorbate levels having nonzero matrix element and one state occupied and another unoccupied can participate in an optical transition and hence may produce a a distinctive feature in $\Delta\epsilon_2$. According to the nature of the electronic states contributing to absorption, the peaks in $\Delta\epsilon_2$ can be grouped into (1) bulklike peaks, (2) surface resonances, and (3) adsorbate-induced features.

1. *Interband transitions: Bulklike peaks*

The bulklike peaks, with positive contributions to $\Delta\epsilon_2$, are located at 1.0, 1.8, 3.3, and 5.0 eV (Fig. 4). At these energies structure appears in the bulk dielectric function. The bulklike peaks were also observed for H, O, and CO adsorption on W(110). They are caused by a transfer in transition probability between resonance levels and band states.[11]

The existence of these peaks in $\Delta\epsilon_2$ can be explained by assuming that S for the clean W surface has two contributions. The first term contributes the strength of all optical transitions involving surface or resonance levels. The second one is the sum of the transition probabilities of all the interband transitions. A different value of S is associated with the chemisorption system because the number of valence electrons changes upon adsorption. As a result, a third term, reflecting all optical transitions involving adsorbate states, appears. Furthermore, some of the surface states that existed for the clean surface are quenched upon chemisorption, and their strength is redistributed. The strength associated with the optical transitions between quenched surface states can go either to interband transitions or to transitions involving adsorbate states until the sum rule is fulfilled. If the transition probability of a resonance state goes into a band to band excitation, a positive peak (bulklike) appears in $\Delta\epsilon_2$ at the same energy as in the bulk dielectric function.

When the transition probability that for the clean surface is associated with a resonance state goes upon chemisorption into an adsorbate state, a bulklike peak, close by in energy, is likely to be missing. As an example, let us consider the 3.3- and 5.0-eV peaks not observed in $\Delta\epsilon_2\langle 001\rangle$ and $\Delta\epsilon_2\langle 1\bar{1}0\rangle$, respectively. The 3.3-eV peak is mainly due to transitions between bands 3 and 4 (in the notation of Ref. 22) along the line PH (Fig. 8). Two resonance levels appear along the line PH for the clean

W surface at the edge of the gap between bands 3 and 4 (dashed lines in Fig. 8). Upon chemisorption the resonance state below E_F disappears,[25] the resonance level above E_F is shifted,[12] and part of the low coverage absorbate state is induced along PH.[26] The strength, that for the clean surface is associated with optical transitions between the resonance states, is transferred, after adsorption, to transitions from the adsorbate state. As a result, the strength of the interband transition does not change and the 3.3-eV peak is missing for $\Delta\epsilon_2\langle 001\rangle$. However, the 3.3-eV peak is observed in $\Delta\epsilon_2\langle 1\bar{1}0\rangle$ because the orbital character of the adsorbate state wave functions is such that the matrix element is almost zero for an electric field along the $\langle 1\bar{1}0\rangle$ direction.

The bulklike peak in $\Delta\epsilon_2\langle 1\bar{1}0\rangle$ at 5.0 eV behaves in a similar way. It is associated with transitions from bands 2 to 4 (Refs. 22 and 11) around the Γ point where the high-coverage hydrogen state appears upon chemisorption.[27]

2. *Resonance states*

The localized states characteristic of the metal surface (surface and resonance levels) are highly sensitive to chemisorption.[23,24] Upon adsorption, they can either remain unchanged, disappear or shift in energy with or without a significant change in their orbital character.[24] The quenching of surface states upon adsorption results in the disappearance of optical transitions associated with the spectrum of the clean W surface. Consequently, a negative contribution is observed in $\Delta\epsilon_2(\omega)$.

The minima at 1.4 eV in $\Delta\epsilon_2\langle 001\rangle$ and $\Delta\epsilon_2\langle 1\bar{1}0\rangle$ (Fig. 4) are due to the quenching upon hydrogen adsorption of two surface resonances.[11] These dips result from the quenching of optical transitions between an occupied resonance state[8,9] and an unoccupied resonance level.[11] The initial electronic state was extensively studied by Holmes *et al.*[25] Their angle-resolved photoemission experiments showed that this state exists over most of the SBZ with the same orbital character and that it gives rise to lobes at 45° to the (110) surface plane along the $\langle 010\rangle$ and $\langle 100\rangle$ directions; thus, the character of the occupied resonance level is yz when referred to the right-handed coordinate system ($\langle 001\rangle$, $\langle 1\bar{1}0\rangle$, $\langle 110\rangle$). The energy of the final state (E_f) is determined by combining UPS and SRS data. However, the knowledge of the final-state energy is not enough information to determine the position of the state along different symmetry lines in the PBS because $\Delta\epsilon_2$ is a sum over all possible contributions in the SBZ. For this particular system, the position of the initial state is known from both theoretical[25] and experimental[8,9,25] studies. These data and the energy and dispersion of the SRS minima make it possible to infer the position of the final state in the PBS. The location of the unoccupied resonance level in the SBZ is shown in Fig. 8 (dashed lines above the Fermi level).

The azimuthal dependence of the matrix element, which follows from the angular dependence of $\Delta\epsilon_2$ at 1.4 eV, serves to determine the possible orbital combinations of the unoccupied resonance state. The position and the symmetry properties of the resonance states in the PBS restricts the possible mixing of the wave functions. As an example, we consider the line ΓH. The symmetry operations along this direction are reflection with respect to the $\langle 1\bar{1}0\rangle$ axis and the identity. It follows that yz can only mix with xy and x^2-y^2 can mix with $3z^2-r^2$. Since the dipole moment selection rules specify the allowed optical transitions from a specific initial state, the orbital character of the final state can be predicted along symmetry lines of the SBZ for an electric field along the $\langle 1\bar{1}0\rangle$ and $\langle 001\rangle$ directions. In accordance with the UPS experiments we assume that the initial state along the line ΓH is a mixture of yz and xy. The selection rules show that when the electric field is along the $\langle 001\rangle$ direction the final state, along ΓH, must also be a mixture of yz and xy. If the electric field is along the $\langle 1\bar{1}0\rangle$ direction, the final state must be x^2-y^2 and/or $3z^2-r^2$. Clearly, symmetry and selection rules are powerful tools to reduce a large initial set of wave functions to a few allowed ones. To choose the correct orbital character of the states from the remaining possibilities a calculation of the matrix elements is done for the different directions of the electric field.

B. Orbital character of the resonance states

In a tight-binding (TB) approximation the initial- and final-state wave functions are

$$\psi_i^k(\vec{r})=\sum_{R,m} a_m(\vec{k})\phi_m(\vec{r}-\vec{R})e^{i\vec{k}\cdot\vec{R}} \tag{10}$$

and

$$\psi_f^k(\vec{r})=\sum_{R',m'} b_{m'}(\vec{k})\phi_{m'}(\vec{r}-\vec{R}')e^{i\vec{k}\cdot\vec{R}'}, \tag{11}$$

where R refers to the lattice sites and m is the projection of the angular momentum l. Since only d wave functions are considered ($l=2$), m varies between -2 and 2. The matrix element is

$$M_{if}^k(r)=\langle\psi_i^k(\vec{r})\,|\,\vec{r}\,|\,\psi_f^k(\vec{r})\rangle$$

$$=\sum_{R;m,m'} a_m(\vec{k})b_{m'}(\vec{k})e^{i\vec{k}\cdot\vec{R}}\langle\phi_{m'}^2(\vec{r})\,|\,\vec{r}\,|\,\phi_m^2(\vec{r}-\vec{R})\rangle. \tag{12}$$

Equation (12) shows that the total matrix element

is a linear combination of matrix elements between two d wave functions, one of which is centered at the origin and the other one at $\vec{R}$. To express both wave functions in the same coordinates, $\phi_m(\vec{r}-\vec{R})$ is expanded about the origin. $\phi_m(\vec{r}-\vec{R})$, a pure d-like wave function at $\vec{R}$, can be represented as a sum of d and non d-like contributions at the origin. However, the only nonzero terms of the matrix elements are those between the p and f-like contribution in the expansion of ϕ_m and $\phi_{m'}$. The following expansion in spherical harmonics about the origin, obtained by Pettifor,[28] was used in the calculation:

$$\phi^2_{m'}(\vec{r}-\vec{R}) = R^2(\vec{r}')Y_{2m'}(\theta',\phi') = \sum_{l'',m''} \bar{R}_{l''}(\vec{r})E_{l''m'',2m'}(\vec{R})Y_{l''m''}(\theta,\phi)\,.$$

The coefficients $E_{l''m'',2m'}$ are related to the relative weight of the l'' component in the expansion of a d wave function about the origin. These coefficients, functions of the Slater-Koster energy integrals,[29] depend on the overlap parameters $pd\pi$ and $pd\sigma$ and the direction of $\vec{R}$. The resonance is assumed to be localized on the first layer of W. This approximation, which is supported by theoretical calculations,[23,24] limits the number of $E_{l''m'',2m'}$ coefficients that contribute to absorption to only those terms that are nonzero on the surface plane.

As an example, the matrix element for an electric field along the $\langle 001\rangle$ direction is calculated along the line ΓH:

$$M^{\langle 001\rangle}_{\Gamma H} = \sum_{R;\,m,\,m'} a_m b_{m'} e^{i\vec{k}\cdot\vec{R}} \frac{\bar{R}_1}{2}\Big(E_{1\,m-1,2m'}(\vec{R})\int_{-1}^{1} P^m_2(z)(1-z^2)^{1/2}P^{m-1}_1(z)dz + E_{1\,m+1,2m'}(\vec{R})\int_{-1}^{1} P^m_2(z)(1-z^2)^{1/2}P^{m+1}_1(z)dz\Big)\,. \tag{13}$$

As explained in Sec. IV A, the initial and final states are linear combinations of yz and xy. Then, the nonzero coefficients in Eq. (13) are $a_{\pm1}$, $a_{\pm2}$, $b_{\pm1}$, and $b_{\pm2}$, which may be written in the form

$$a_1 = a_{xz} + ia_{yz},\quad a_2 = a_{x^2-y^2} + ia_{xy},\qquad a_{-1} = a_{xz} - ia_{yz},\quad a_{-2} = a_{x^2-y^2} - ia_{xy}\,. \tag{14}$$

It can be seen that a_{xz} and $a_{x^2-y^2}$ in Eq. (14) are zero because the corresponding wavefunctions cannot mix with yz, xy along the line ΓH.

In the calculation of $M\langle 001\rangle_{\Gamma H}$ we used the tabulated coefficients E,[29] restricted the sum over lattice sites to the near neighbors, and used the relation $k_{\Gamma H} = (2\pi/a)(x,0)$, where a is the lattice constant and $0 < x < \frac{3}{4}$. This gives

$$M^{\langle 001\rangle}_{\Gamma H} = \alpha a_{xy} b_{yz} \sin\pi x \frac{pd\pi}{\sqrt{3}} \quad (\alpha = \text{const})\,.$$

$M^{\langle 1\bar{1}0\rangle}_{\Gamma H}$ is also found to be proportional to α, a_{xy}, and $\sin\pi x$. As a result, the ratio of the matrix elements along ΓH becomes

$$M\langle 001\rangle / M\langle 1\bar{1}0\rangle = Ab_{yz}/(A'b_{3z^2-r^2} + B'b_{x^2-y^2})$$

The constants A, A', and B' are proportional to the overlap parameters $pd\sigma$ and $pd\pi$.

The matrix elements along the lines PH and ΓN were also calculated for the electric field in both the $\langle 001\rangle$ and the $\langle 1\bar{1}0\rangle$ directions. It is found that the matrix element, for an electric field along the $\langle 001\rangle$ direction, is proportional to b_{yz} along ΓH, to $b_{x^2-y^2}$ and/or $b_{3z^2-r^2}$ along HP and to b_{xy} along ΓN. The matrix element, for an electric field along the $\langle 1\bar{1}0\rangle$ direction, is proportional mainly to $b_{x^2-y^2}$ (and/or $b_{3z^2-r^2}$) along ΓH, HP, and ΓN.

As shown in Fig. 4, $\Delta\epsilon_2$ is larger for an electric field along $\langle 001\rangle$ than for an electric field along $\langle 1\bar{1}0\rangle$, i.e., $M\langle 001\rangle/M\langle 1\bar{1}0\rangle > 1$. Along the ΓH line, the inequality can be expressed as

$$(Ab_{yz})^2 > (A'b_{3z^2-r^2} + B'b_{x^2-y^2})^2\,,$$

implying a nonzero b_{yz} contribution. Therefore, $b_{3z^2-r^2}$ and $b_{x^2-y^2}$ must be zero because the corresponding wavefunctions cannot mix with yz. As a result, if there is absorption along the line ΓH, the character of the unoccupied resonance must be $b_{yz}yz + b_{xy}xy$ with $b_{yz} \neq 0$. In a similar manner, the orbital character of the unoccupied resonance is determined along other symmetry lines. The calculations show that it is mainly yz along ΓH, yz, and x^2-y^2 (and/or $3z^3-r^2$) along HP, and xy along ΓN.

It is apparent from Fig. 8 that most of the observed adsorption must come from optical transitions between the resonance states along the line HP. This direction has a complete lack of

symmetry except at the points G, P, and H. The resonance level must be pure yz at P and H and $3z^2-r^2$ and/or x^2-y^2 at G (G = midpoint of PH). As a result, the character of the occupied resonance state must be

$$b_{yz}(k)yz + b_{x^2-y^2}(k)(x^2-y^2) + b_{3z^2-r^2}(k)(3z^2-r^2)$$

along PH. The coefficient $b_{yz}(k)$ must decrease on going from P toward G, where it is zero because yz is forbidden, and increase again toward H. $b_{x^2-y^2}(k)$ and $b_{3z^2-r^2}(k)$ vary in the opposite way, since they must be zero at P and H. The presence of the unoccupied resonance state around G would result in a larger absorption for an electric field along the $\langle 1\bar{1}0\rangle$ direction. However, no contribution to absorption exists around G because UPS experiments show that the occupied resonance state does not exist in this region. Then the combination of the b_{yz} component that increases towards P and H and the $b_{x^2-y^2}$, $b_{3z^2-r^2}$ components that decrease towards P and H gives a larger absorption for an electric field along $\langle 001\rangle$ than for the electric field along $\langle 1\bar{1}0\rangle$ direction. Still, the presence of x^2-y^2 and/or $3z^2-r^2$ components are necessary to explain the absorption observed in $\Delta\epsilon_2$ $\langle 1\bar{1}0\rangle$ at 1.4 eV (Fig. 4).

C. Adsorbate features

Hydrogen adsorption on W(110) has been studied previously by a variety of methods. Thermal desorption experiments[30] (TDS) show two peaks that have been associated with two different binding configurations of the adsorbate. The state that appears at high coverages and that desorbs at lower temperatures is labeled β_1, while the state that appears at low coverages and desorbs at higher temperatures is called β_2. However, the TDS data do not permit a distinction between an adsorbate containing two intrinsically different binding states and an adsorbate containing just one state with repulsive interactions between the H atoms. Angle-resolved[27] and wide-collection-angle[26] UPS studies on the H/W(110) system show two peaks. In the former technique the low- and high-coverage hydrogen peaks appear at -2.8 and -4.0 eV,[27] respectively, with respect to E_F. In wide-angle UPS experiments, the hydrogen peaks appear at -2.2 and at -3.9 eV.[26]

SRS shows adsorbate-induced features at 2.6 eV in $\Delta\epsilon_2$ $\langle 001\rangle$ and 5.5 eV in $\Delta\epsilon_2$ $\langle 1\bar{1}0\rangle$ (Fig. 4) and their angular dependence provides a rather direct determination of the transition matrix elements. The 2.6-eV peak shows maximum absorption for an electric field along the $\langle 001\rangle$ direction and a negligible contribution for an electric field along the $\langle 1\bar{1}0\rangle$ direction. The amplitude of the 5.5-eV peak shows the opposite behavior with respect to the direction of the electric field. As for the other features, the energy of the final state is determined by combining SRS and UPS data. The final state associated with optical transitions from the β_2 state is found to be located close to the Fermi level and the final state corresponding to the optical transitions from the β_1 state is located at 1.5 eV above the Fermi level. The analysis of the energy and the dispersion of the UPS peaks give the location of the adsorbate levels along the different symmetry lines in the PBS. It is assumed that the adsorbate states are located in gaps since interactions between the adsorbate states and the d band is expected to broaden the adsorbate states outside gap regions[31] and most optical transitions from such states would not appear as sharp peaks either in UPS or in SRS spectra. This general behavior has been established for other systems; in the case of H/Pd(111), Louie[31] showed that the antibonding hydrogen state disappears into the d band outside gaps. However, the bonding hydrogen state for Pd(111) (Ref. 31) and both the bonding and antibonding state for Mo(100) (Ref. 32) (located below the edge of the d band) extend over all the SBZ. The fact that the adsorbate states for H/W(110) do not extend over all the SBZ is closely related to the particular surface band structure; since adsorbate states appear in the middle of the d band, it is likely that most features are localized in gaps.

The present analysis shows that the high-coverage adsorbate state is located at the edge of the gap around the Γ point. The β_1 state exhibits similar dispersion towards H and N because the corresponding UPS peak appears at the same energy for experiments performed at electron collection cones of 6° and 45°.[26,27] The β_2 state exists in the gap around N toward the point Γ, around Γ towards H and N, and in the gap around H towards P. The state must exist around Γ because an UPS peak is seen in experiments performed at 6° electron collection cone.[27] For an electron collection cone of 54°, the UPS peak is shifted toward lower energies, showing that the state also exists outside Γ. The gaps along ΓN and PH have the appropriate energy to locate parts of the β_2 state.

As mentioned earlier, SRS experiments give the average of the possible contributions over all the surface Brillouin zone. Therefore the β_2 state is expected to appear in $\Delta\epsilon_2$, as it does, at the average energy of the UPS peaks (2.6 eV). This suggests that all pieces of the low-coverage absorbate state contribute to the absorption observed in $\Delta\epsilon_2(\omega)$.

The adsorbate wave functions, as well as the hydrogen adsorption sites, have not been well determined for the H/W(110) system. There are

electron-energy-loss data[33] (ELS) in the literature for hydrogen adsorbed on the (100), (110), and (111) faces of tungsten. The measurements, made in the specular reflection direction, showed one common vibrational frequency for all three crystal orientations. This was interpreted as an indication that H adsorbs directly on top of each W atom. Later ELS experiments[34] for H/W(100), in the off-specular direction, showed three stretching modes, strongly suggesting bridged-site adsorption. Similar data have not yet become available for H/W(110). Recent field emission microscopy (FEM) studies by DiFoggio and Gomer[35] of hydrogen diffusion on W(110) suggests that bridge site is a possible binding configuration.

The results obtained in the present work can be used to determine the geometry of the adsorbate on the surface and the orbital character of the wave functions. The procedure involves an analysis of the angular dependence of the matrix elements and uses group-theoretical arguments and selection rules. A particular geometry of the hydrogen atoms on the surface is chosen in the analysis and the set of wave functions compatible with that configuration is determined. It was assumed that the strong bonding of the hydrogen to the surface comes from the interaction of the H $1s$ and W $5d$ orbitals. By means of group theoretical arguments, the mixing of the d-like and s-like wave functions is determined along the symmetry lines where the adsorbate states are located (as shown in Sec. IV A). The dipole-moment selection rules restrict the possible final state. The matrix elements were calculated within a tight-binding approximation and compared to those obtained experimentally.

The tight-binding wave functions for the H and the initial state are

$$\psi_{1s}(r)=\sum_R c_{1s}e^{i\vec{k}\cdot(\vec{R}+\vec{d})}\phi_{1s}(\vec{r}-(\vec{R}+\vec{d})), \qquad |d|=\begin{cases}0 & \text{on top}\\ \frac{a}{\sqrt{2}} & \text{bridged site}\end{cases}$$

$$\psi_i^k(r)=\sum_{R,m} a_m e^{i\vec{k}\cdot\vec{R}}\phi_m(\vec{r}-\vec{R})+\sum_R c_{1s}e^{i\vec{k}\cdot(\vec{R}+\vec{d})}\phi_{1s}(\vec{r}-(\vec{R}+\vec{d})),$$

where R refers to the lattice sites, m is the projection of the angular momentum, and d is the displacement of the hydrogen atoms with respect to the W atom.

It is found that the β_1 state is a mixture only of $1s$, x^2-y^2, and/or $3z^2-r^2$ for the two models considered. The orbital character does not change with the geometry because the parity of the wave functions along ΓN and ΓH is the same for either configuration.

The character of the final state for transitions from the β_1 state can be determined partially. It can be either yz or x^2-y^2 and/or $3z^2-r^2$. The x^2-y^2 and $3z^2-r^2$ contributions cannot be separated either by group theory or by the TB calculation. A band-structure calculation would be required to determine their relative weight. The final state cannot be xy because b_{xy} must be negligible in comparison to $b_{3z^2-r^2}$ and/or $b_{x^2-y^2}$. Since x^2-y^2 and $3z^3-r^2$ cannot mix with xy they must be zero and, consequently, xy must be zero also. An xz contribution in the orbital character of the unoccupied resonance state could not be determined because the associated $E_{l''m'',2m'}$ are always zero due to the restriction of the calculation to the first layer of tungsten. The error introduced by this assumption is probably small because about 80% of the resonance states are localized in the surface layer. The smallness of the xy component supports our assumption that the unoccupied resonance state extends only over part of ΓN. If the resonance existed around Γ towards N, it would be a favorable final state for optical transitions from the β_1 state. Since it was found that its character is mainly xy along the line ΓN, a large absorption would have had to appear in $\Delta\epsilon\ \langle 001\rangle$, which is opposite to the observed behavior.

Although this study of the high-coverage H state does not determine the adsorption site, it does determine the orbital character of the adsorbate state and restricts the character of the final state. A more detailed discussion is possible for the low-coverage state, and two possible models will be considered. In the first each adatom is assumed to occupy a bridge site,[13] in the second the adatoms are located directly on top of the W atoms.

At low coverages the orbital character of the adsorbate state is $1s$, yz in the gaps around N and H. Analysis of the calculated matrix elements shows that if hydrogen is in bridged sites, the final state of the optical transition must have the same orbital character as the unoccupied reso-

nance state. The part of the β_2-H state that is centered about G (midpoint of PH) has mainly x^2-y^2 and/or $3z^2-r^2$ orbital character. It may mix with yz toward P and H. The calculation showed that, for an electric field along the $\langle 1\bar{1}0\rangle$ direction, the main contribution to absorption comes from x^2-y^2 and/or $3z^2-r^2$ and yx with opposite signs. Although x^2-y^2 and/or $3z^2-r^2$ components give absorption for either direction of the electric field, the yz adsorption compensates the x^2-y^2, $3z^2-r^2$ component for an electric field along the $\langle 1\bar{1}0\rangle$ direction. As a result, the matrix element along the $\langle 1\bar{1}0\rangle$ direction is very small. Therefore, the angular dependence observed in $\Delta\epsilon_2(\omega)$ can be explained if hydrogen is located in bridged sites and the final state of the optical transition is the unoccupied resonance state. The presence of the hydrogen on the surface also seems to shift the resonance state which after chemisorption is located very close to the Fermi level. It is interesting to note that Louie[31] and Perker *et al.*,[32] who calculated the band structures of hydrogen chemisorbed on Pd(111) and Mo(100), respectively, found that in both systems, hydrogen adsorption shifts some surface states and resonance levels toward lower energies.

If, instead, hydrogen is assumed to occupy on top sites, the β_2 state must result from a mixing of the hydrogen $1s$ orbital with x^2-y^2 and/or $3z^2-r^2$ over the whole SBZ. At the point G as well as at P and H, this is the only possible mixing. In this bonding configuration, the final state must have a large yz component around G where the β_2 state is centered. The orbital character of the unoccupied resonance state around G is x^2-y^2, $3z^2-r^2$ and it cannot change due to symmetry considerations (G has inversion symmetry). Therefore, an entirely new state would have to exist at the Fermi level with the required yz orbital character. Furthermore, the unoccupied resonance state would have to disappear simultaneously or an extra peak should be observed in $\Delta\epsilon_2(\omega)$.

V. SUMMARY

The present study shows that surface relectance spectroscopy is well suited to the study of the electronic properties of surfaces. Among the advantages of SRS are that it is neither destructive as a surface probe nor limited to an UHV environment, as electron spectroscopies are. The method is particularly useful in the detection and study of small anisotropies in the optical properties of chemisorbed systems. For such systems SRS gives a rather direct determination of the matrix elements, the orbital character of the wave functions and the geometry of the adsorbate on the surface plane. The main limitation is that SRS gives the joint density of states. Consequently, other results (in particular UPS) are necessary for the analysis of an absorption spectrum. Also, the interpretation of the data requires an elaborate analysis.

Our results for H/W(110) show that both clean and adsorbed surfaces have rectangular symmetry. A surface resonance has been found above the Fermi level separating from the gap between bands 3 and 4. The unoccupied resonance and the associated optical transitions are located in the PBS. Its orbital character, and the behavior of the resonance upon hydrogen adsorption have been determined. It was found that bridged sites are favorable hydrogen adsorption sites. The analysis shows that SRS data can be explained by considering equivalent bridge sites.

To conclude, SRS can be an important surface technique because it allows the simultaneous study of adsorbate bonding configurations and the corresponding features in the surface band structure. Such a study has resulted in a rather detailed description of the electronic properties of the H/W(110) system.

ACKNOWLEDGMENTS

We are indebted to D.R. Grempel for his interest in and his many contributions to this work. We also thank P.J. Feibelman for useful suggestions on the manuscript. This work was supported by the Materials Research Laboratory at Brown University funded by the National Science Foundation.

---

*Present address: Department of Physics, University of Pennsylvania, Philadelphia, Pennsylvania.

[1]G. W. Rubloff, J. Anderson, and P. J. Stiles, Surf. Sci. 37, 75 (1973).

[2]G. W. Rubloff, J. Anderson, M. A. Passler, and P. J. Stiles, Phys. Rev. Lett. 32, 667 (1974); J. Anderson, G. W. Rubloff, M. A. Passler, and P. J. Stiles, Phys. Rev. B 10, 2401 (1974).

[3]M. A. Passler and P. J. Stiles, J. Vac. Sci. Technol. 15, 2, March/April (1978).

[4]J. E. Cunningham, D. Greenlaw, C. P. Flynn and J. L. Erskine, Phys. Rev. Lett. 42, 328 (1979).
[5]G. W. Rubloff and J. L. Freeouf, Phys. Rev. B 17, 4680 (1978).
[6]E. W. Plummer, in *Interactions on Metal Surfaces*, Vol. 4 of *Topics in Applied Physics*, edited by R. Gomer (Springer, New York, 1975), p. 143.
[7]B. Feuerbacher and B. Fitton, in *Electron Spectroscopy for Surface Analysis*, edited by H. Ibach (Springer, New York, 1977).
[8]B. Feuerbacher and N. Egede Christensen, Phys. Rev. B 10, 2373 (1974).
[9]B. Feuerbacher and B. Fitton, Phys. Rev. Lett. 30, 923 (1973).
[10]J. D. E. McIntyre, in *Advances in Electrochemistry and Electrochemical Engineering*, edited by Paul Delahay and Charles Tobias (Wiley, New York, 1973), Vol. 9.
[11]G. B. Blanchet and P. J. Stiles, Phys. Rev. B 21, 3273 (1980).
[12]G. B. Blanchet, P. J. Estrup, and P. J. Stiles, Phys. Rev. Lett. 44, 171 (1980); G. B. Blanchet, P. J. Estrup, and P. J. Stiles, Bull. Am. Phys. Soc. 24, 339 (1979) and unpublished work.
[13]D. M. Kolb, R. Kotz, and T. Yamamoto, Surf. Sci. 87, 20 (1979).
[14]M. A. Passler, Ph.D. Thesis, Physics Department, Brown University, 1977 (unpublished).
[15]The electronics and feedback circuit are similar to those described in U. Gerhart and G. W. Rubloff, Appl. Opt. 8, 305 (1969).
[16]P. J. Feibelman, Phys. Rev. B 12, 1319 (1975); 14, 762 (1976).
[17]A. Bagchi and A. K. Rajagopal, Solid State Commun. 31, 127 (1979).
[18]J. D. E. McIntyre and D. E. Aspnes, Surf. Sci. 24, 417 (1971).
[19]L. V. Nomerovannaya, M. M. Kirillowa, and M. M. Noskov, Zh. Eksp. Teor. Fiz. 60, 748 (1971) [Sov. Phys.—JETP 33, 405 (1971)].
[20]J. M. Ziman, *Principles of the Theory of Solids* (Cambridge University Press, Cambridge, 1964).
[21]J. B. Restorff, Ph.D. Thesis, Physics Department, University of Maryland, 1976 (unpublished).
[22]N. Egede Christensen, and B. Feuerbacher, Phys. Rev. B 10, 2349 (1974).
[23]G. P. Kerker, K. M. Ho, and Marvin L. Cohen, Phys. Rev. Lett. 40, 1493 (1978).
[24]S. G. Louie, Phys. Rev. Lett. 40, 1525 (1978).
[25]N. W. Holmes, D. A. King and J. E. Inglesfield, Phys. Rev. Lett. 42, 394 (1979).
[26]E. W. Plummer, T. V. Vorburger, and C. E. Kuyatt, in *Progress in Surface Science*, edited by Sydney G. Davison (Pergamon, New York, 1976), Vol. 7, p. 149.
[27]B. Feuerbacher and B. Fitton, Phys. Rev. B 8, 4890 (1973).
[28]D. G. Pettifor, J. Phys. C 5, 97 (1972).
[29]J. C. Slater and G. F. Koster, Phys. Rev. 94, 1498 (1954).
[30]L. D. Schmidt, in *Interactions on Metal Surfaces*, Vol. 4 of *Topics in Applied Physics*, edited by R. Gomer (Springer, New York, 1975), p. 63.
[31]S. G. Louie, Phys. Rev. Lett. 42, 476 (1979).
[32]G. P. Perker, M. T. Yin, and M. L. Cohen (unpublished).
[33]C. Bachk, B. Feuerbacher, B. Fitton, and R. F. Willis, Phys. Lett. 60A, 145 (1977).
[34]W. Ho, R. F. Willis, and E. W. Plummer, Phys. Rev. Lett. 40, 1463 (1978).
[35]R. Di Foggio and R. Gomer, Phys. Rev. Lett. 44, 1258 (1980).

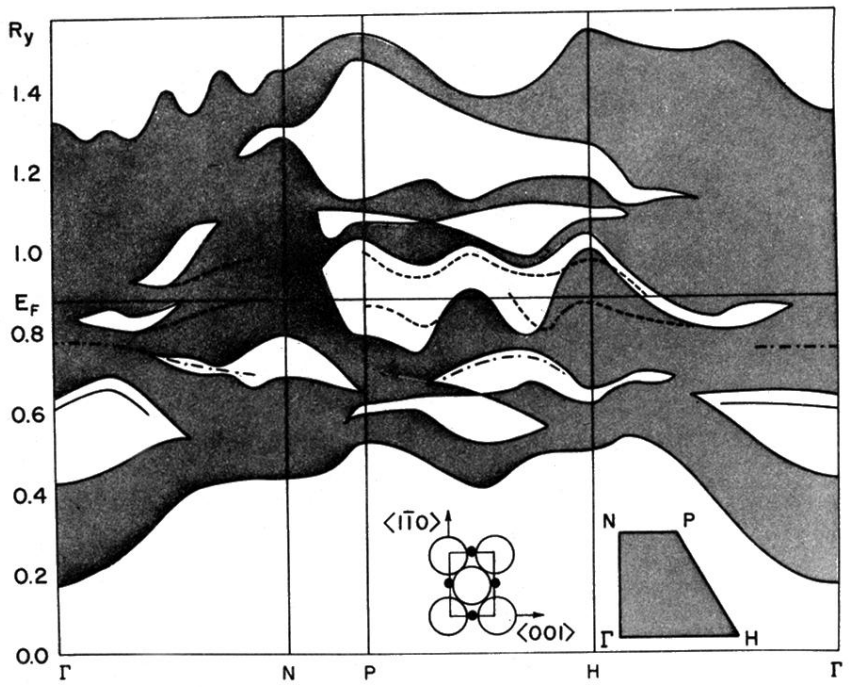

FIG. 8. Projected band structure for the W(110) surface. Dashed lines refer to the surface resonances, solid lines to the high-coverage hydrogen state and dashed-dotted lines to the low-coverage hydrogen state. Insets show the corresponding SBZ and the bridge-site position of the atoms (solid circles) on the direct W lattice (empty circles).